

Raman spectroscopy and normal-mode assignments for $Ba_2MCu_3O_x$ ($M = Gd, Y$) single crystals

D. M. Krol, M. Stavola, W. Weber,* L. F. Schneemeyer, J. V. Waszczak,
S. M. Zahurak, and S. G. Kosinski

AT&T Bell Laboratories, 600 Mountain Avenue, Murray Hill, New Jersey 07974-2070

(Received 14 August 1987)

Single crystals of superconducting $Ba_2MCu_3O_x$ ($M=Y, Gd$) have been used for a study of the polarization dependence of the Raman spectra so as to better understand the lattice dynamics and the role of O defects in these materials. Several prominent vibrational bands have strong polarization dependence and can all be attributed to specific modes with A_g symmetry. Broad features between 500 and 600 cm^{-1} are suggested to be related to O vacancy disorder.

Since the discovery of high- T_c superconductivity several workers have reported the Raman spectra of $Ba_2MCu_3O_7$ ($M=rare\text{-earth element or Y}$).¹⁻⁹ From the Raman spectra information about the lattice dynamics, O vacancy disorder, and possible contaminant phases can be derived. However, the reported Raman spectra show marked differences and the assignments of the vibrational modes in the various studies disagree. Here, in order to make more definitive Raman assignments, we have measured the polarization dependence of the Raman spectra of single crystals of $Ba_2YCu_3O_x$ and $Ba_2GdCu_3O_x$. Several previously observed modes show strong polarization dependence, which leads to their assignment as A_g modes. Broad features between 500 and 600 cm^{-1} have little polarization dependence and appear to be related to oxygen vacancy disorder.

In an earlier paper¹ we have reported Raman and infrared absorption (ir) data on sintered powder pellets of composition $Ba_2YCu_3O_x$ with $6 \leq x \leq 7$. For $x \geq 6.5$ these materials are superconducting and their crystal structure is orthorhombic.^{10,11} For $x \leq 6.5$ they are tetragonal and semiconducting.^{12,13} The strongest Raman band, which is located at 500 cm^{-1} in the orthorhombic phase and at 470 cm^{-1} in the tetragonal phase, was assigned to the O(1) symmetric stretching vibration (A_g symmetry). The structural notation follows that of Siegrist *et al.*¹¹ and is consistent with our Ref. 1. Raman bands were also observed at 590 and 430 cm^{-1} . The former was assigned to B_{2g} and B_{3g} Cu-O stretching modes and the latter could not be assigned without information about its polarization properties.

The effect of the isotopic substitution, ^{18}O for ^{16}O , upon the Raman spectrum has been measured.^{2,9} The bands at approximately 590, 500, 430, 340 cm^{-1} , and also a band at 635 cm^{-1} showed a pronounced decrease in frequency in the ^{18}O substituted sample, demonstrating that these modes all are oxygen vibrations. Further, it is now known that different annealing procedures modify the dependence of the orthorhombic to tetragonal transition upon oxygen content.¹⁴ In a study of $Ba_2YCu_3O_x$ samples⁹ coannealed in vacuum with zirconium foil it was shown that the intensity of the 590- cm^{-1} band increased monotonically as additional oxygen vacancies were introduced over the range $7 > x > 6.3$ all in the orthorhombic structure. Most Raman measurements have been done on

ceramic powder samples except for one study on very small, 10–30- μm size crystals.³ In this work, however, not all the modes found in the powders have been observed and some of the results disagree with the work to be reported here.

For our studies millimeter-size crystals were grown as described by Schneemeyer *et al.*¹⁵ After annealing for several hours in oxygen at 500°C, they are superconducting with a T_c around 90 K. Some of the crystals were further annealed in O_2 for 72 h at 500°C in order to maximize the oxygen content, whereas others were annealed in N_2 for 2 h at 700°C to obtain more oxygen-deficient, tetragonal compositions. All samples were thin platelets with the c axis normal to the basal plane. Many crystals had square corners with a and b axes parallel to these edges; however, a - b microtwinning precludes study of the a - b anisotropy.^{15,16} Control of the oxygen content in the single crystals is not as straightforward as in the sintered pellets because the oxygen diffusion distance is smaller compared to the crystal size.

The Raman setup consisted of an Instruments SA MOLE Raman microprobe, which is described in more detail elsewhere.¹⁷ Measurements were done both with the Raman microscope (backscattering) and in the macrochamber (grazing incidence) using either 514.5 or 488.0 nm excitation. The laser power was less than 100 mW in the macrochamber and less than 3 mW in the microscope. The instrumental resolution was 5 cm^{-1} . For the Raman measurements we have used crystals with $M=Gd$ and Y . Crystals with similar annealing treatment gave similar Raman spectra for the Y - and Gd -containing crystals.

In Fig. 1 we present the zz spectra of three $Ba_2YCu_3O_x$ crystals with different oxygen content. For all samples a very strong peak is observed in the 500- cm^{-1} region whose position and shape depend on sample treatment. In going from the oxygen-rich crystal (A) to the oxygen-deficient crystal (C) the 500- cm^{-1} peak shifts from 500 (O) to 472 (T) cm^{-1} where the orthorhombic or tetragonal structures are indicated in parentheses. Similar behavior was reported in Ref. 1. Crystal B is an intermediate case. The 500- cm^{-1} band is broader than for crystal A. Two weaker peaks at 435 and 140 cm^{-1} are also observed.

In Fig. 2 for the xx ($=yy$) geometries (which cannot be distinguished because of the twinning) weak features are

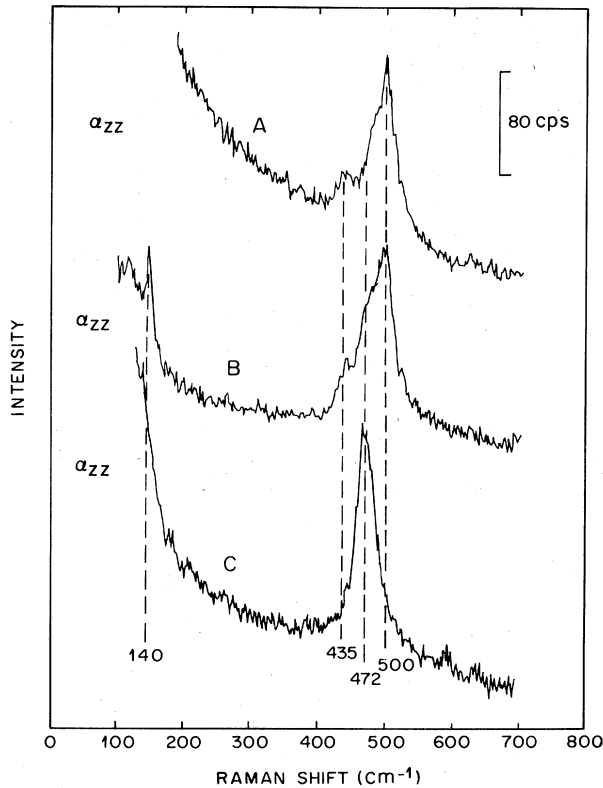


FIG. 1. Raman spectra of various $\text{Ba}_2\text{YCu}_3\text{O}_x$ crystals with incident and scattered light propagating perpendicular to the c axis of the crystal ($\mathbf{k}_i \parallel \mathbf{k}_s \perp \mathbf{c}$) and both polarizations parallel to the c axis ($\mathbf{e}_i \parallel \mathbf{e}_s \parallel \mathbf{c}$). A: $\text{Ba}_2\text{YCu}_3\text{O}_x$, annealed for 72 h in O_2 at 500°C . B: $\text{Ba}_2\text{YCu}_3\text{O}_x$, annealed for 2 h in O_2 at 500°C . C: $\text{Ba}_2\text{YCu}_3\text{O}_x$, annealed for 2 h in N_2 at 700°C .

observed at 335 and around 500 cm^{-1} . No peaks are seen in the xy and $zx (=zy)$ geometries. On the basis of group theory no modes are predicted for the xy geometry (i.e., there are no B_{1g} modes), but the Raman-active B_{2g} and B_{3g} modes¹ should be observed in the $zx (=zy)$ geometry.

In a further attempt to observe the B_{2g} and B_{3g} modes we have done several grazing incident experiments on the crystal face normal to the c axis with the scattered light collected at 90° . In this scattering geometry more bands are observed, but the polarization information is not as selective because the incident beam cannot be perfectly normal to the c axis [cf. Figs. 3(a) and 3(b)]. The 335-cm^{-1} peak is again observed and its presence is consistent with its xx character. This feature is also weakly observed in the zx geometry, most probably because of imperfect sample alignment. The 140-cm^{-1} band which was also observed in Fig. 1 (zz) is now also present as an xx feature. It was not seen in Fig. 2 (xx) because of the high background scattering.

There is also a very weak band at 230 (O)/ 220 (T) cm^{-1} that is observed in some of our spectra. It is primarily of xx character and its position depends on the annealing conditions. Finally there are some broad features in the $500\text{--}600\text{-cm}^{-1}$ region, whose intensity (relative to the 335-cm^{-1} band) varies from sample to sample.

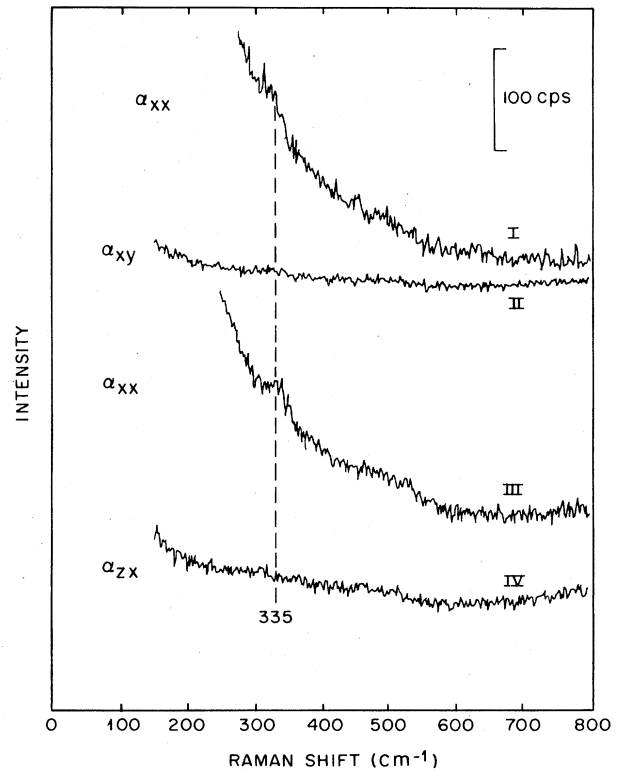


FIG. 2. Raman spectra of various $\text{Ba}_2\text{M(Cu}_3\text{)O}_x$ crystals in backscattering geometry. I: $\text{Ba}_2\text{GdCu}_3\text{O}_x$ annealed as crystal A, $\mathbf{k}_i \parallel \mathbf{k}_s \parallel \mathbf{c}$ and $\mathbf{e}_i \parallel \mathbf{e}_s \parallel \mathbf{a}$. II: As I, but $\mathbf{e}_i \perp \mathbf{e}_s$ and $\mathbf{e}_i \parallel \mathbf{a}$. III: $\text{Ba}_2\text{GdCu}_3\text{O}_x$, annealed as crystal C, $\mathbf{k}_i \parallel \mathbf{k}_s \perp \mathbf{c}$ and $\mathbf{e}_i \parallel \mathbf{e}_s \perp \mathbf{c}$. IV: As III, but $\mathbf{e}_i \perp \mathbf{e}_s$ and $\mathbf{e}_i \parallel \mathbf{c}$.

We discuss the assignments of the various Raman peaks. Group theory shows that there are 15 Raman active modes, with 5 of A_g , 5 of B_{2g} , and 5 of B_{3g} symmetry. We use the orthorhombic notation both for the orthorhombic and tetragonal structures as in Ref. 1, although the orthorhombic B_{2g} and B_{3g} modes become degenerate E_g modes in the tetragonal structure. In going from the orthorhombic ($Pmmm$) to the tetragonal ($P4/mmm$) structure three ir-active vibrational models disappear, but the number of Raman modes remains unchanged.

Raman scattering from A_g symmetry modes is allowed for xx , yy , or zz geometries. Raman scattering from the B_{2g} and B_{3g} modes is allowed for xz , zx , yz , and zy geometries. All of the features that we have observed that have strong polarization dependence are consistent with A_g symmetry. A summary of our results and suggested assignments of the A_g modes are given in Table I. The assignments are justified below. Note that all the A_g mode displacements are along the z axis. Further, because the Raman-active modes are gerade, only atoms which are not inversion centers can be involved. This excludes $\text{Cu}(1)$, $\text{O}(4)$, and Y . In realistic force-constant models the A_g modes will be mixed, but usually one specific mode character dominates if the modes differ substantially in frequency.

We assign the $500/472\text{-cm}^{-1}$ band to the axial $\text{O}(1)$

TABLE I. A_g mode Raman frequencies, observed polarizations, and suggested mode assignments for $Ba_2YCu_3O_x$.

Frequency (cm^{-1})	Polarization	Assignment
500 (O)/472 (T)	zz	O(1) axial symmetric stretching
435	zz	O(2),O(3) in-phase bond bending
335	xx	O(2),O(3) out-of-phase bond bending
230 (O)/220 (T)	xx	Cu(2) axial symmetric stretching
140	zz,xx	Symmetric stretching of Ba planes

stretching mode because of its high frequency, isotope shift, and zz polarization. The axial O(1) motion is expected to strongly modulate the polarizability only along z. The dependence of the peak position on the oxygen content also supports this assignment, because this mode should be most strongly influenced by the elongation of the c axis as the oxygen content decreases.¹⁰

The assignment of the 435- and 335- cm^{-1} bands to the Cu(2)-O(2,3) bending modes is suggested by the oxygen isotope shift and our previous lattice dynamical calculations.¹¹ A problem with this assignment is the large splitting between these bands and the high frequency of the 435- cm^{-1} mode which are not apparent from short-range

force-constant models. The 435- cm^{-1} band has zz character, while the 340- cm^{-1} band has xx character. This leads us to assign the 435- cm^{-1} band to a Cu(2)-O(2,3) bending mode in which O(2) and O(3) neighbors move in phase. Such motion would be expected to strongly modulate the polarizability along z because the effects of the O(2) and O(3) displacements add. When O(2) and O(3) neighbors move out of phase the effects of their displacement along z cancel; thus we assign this mode to the 340- cm^{-1} band (xx). The splitting may be due to the Coulomb repulsion between the negatively charged O(2) and O(3) ions, which reduces the frequency of the out-of-phase motion and enhances that of the in-phase motion.

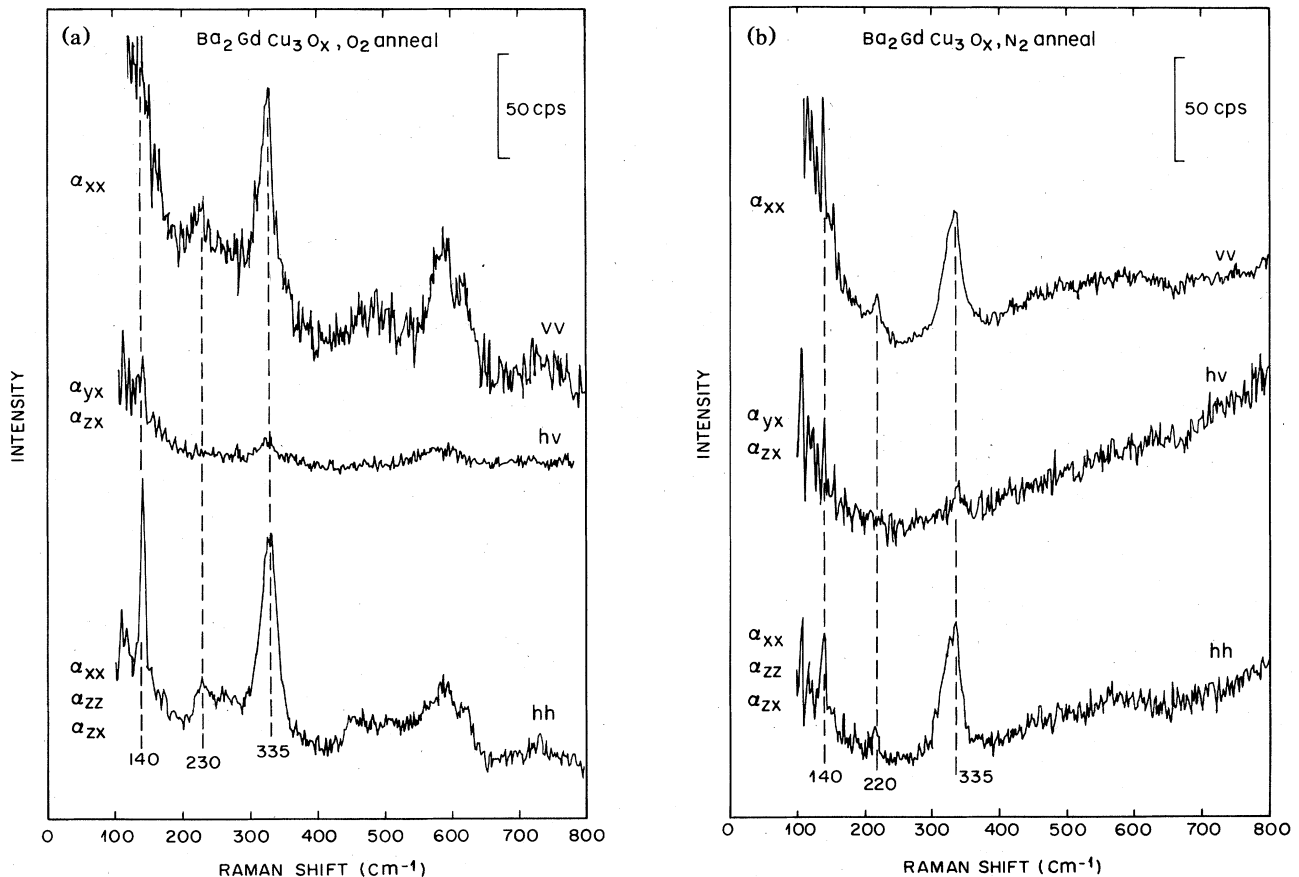


FIG. 3. Grazing incident Raman spectra of $Ba_2GdCu_3O_x$, (a) annealed for 72 h in O_2 at $500^\circ C$ and (b) annealed for 2 h in N_2 at $700^\circ C$. $k_i \perp k_s$, both in $ac (=bc)$ plane of crystal. vv: e_i and $e_s \perp ac$ scattering plane. hv: e_i in ac scattering plane, $e_s \perp ac$ scattering plane. hh: e_i and e_s in ac scattering plane.

The weak 230(O)/220(T) line and 140-cm⁻¹ line cannot be unambiguously assigned. On the basis of the short-range lattice-dynamical models one would assign the 220-cm⁻¹ feature to the Cu(2) mode and the 140-cm⁻¹ line to the Ba mode; the shift of the 230/220-cm⁻¹ band to lower energy in going from the orthorhombic to the tetragonal structure is in agreement with this assignment, although one would have expected this mode to have a strong *zz* character, which is not observed. The 140-cm⁻¹ line is very sharp, and this observation gives further support for its assignment to the Ba vibration. Generally, Raman scattering in metals gives the result that all those modes have large linewidths which involve modulations of the "metallic" bonds.¹⁸ The Cu–O superconductors are no exception, as far as their Cu–O vibrations are concerned. Since the Ba atoms are basically inert donor ions, and thus no Ba valence electron orbitals are involved in the metallic bands, one should indeed expect Raman lines almost as sharp as in ionic insulators.

The assignment of the 500–600-cm⁻¹ features is less straightforward. In our previous work¹ we had assigned a band at 590 cm⁻¹ to the highest frequency, Cu(2)–O(2,3) stretching, *B*_{2g} and *B*_{3g} modes. Such modes should be observed only in *zx* (or *zy*) polarization. Our single-crystal results show no clear evidence for *B*_{2g} and *B*_{3g} modes and specifically do not allow us to assign the 500–600-cm⁻¹ features exclusively to *B*_{2g} and *B*_{3g} modes because they are also seen for *xx* polarization [(Fig. 3(a)]. We note that the *B*_{2g} and *B*_{3g} modes would be expected to be weak because they involve interplanar coupling.

Therefore, because this band is very broad and has little polarization dependence, we suggest that it is due to O vacancy disorder that arises from deviation from the stoichiometric O₇ or O₆ endpoints. Such disorder might make lattice modes with *q* ≠ 0 Raman allowed, so that the spectrum reflects the one-phonon density of states, and might also give rise to additional local defect modes.

Such an assignment is consistent with the increase in intensity of this band as the number of oxygen vacancies is increased. This was suggested elsewhere⁹ for sintered pellets in which the O vacancy content could be more precisely controlled. In our crystals the defect-induced band is more intense for the O₂ annealed samples, suggesting a larger deviation from a stoichiometric composition for these crystals. This is consistent with our spectra (Fig. 1) which show a relatively sharp 472-cm⁻¹ feature in the N₂ annealed sample (hence close to the O₆ composition) and a broader 500-cm⁻¹ feature for the O₂ annealed sample.

In summary, we have determined the polarization dependence of the Raman bands in Ba₂MCu₃O_x crystals. Five *A*_g modes with strong polarization dependence are found at 500(O)/472 (T), 435, 335, 230 (O)/220 (T), and 140 cm⁻¹, all of which are assigned. The results provide evidence that the features observed between 500–600 cm⁻¹ result from oxygen vacancy disorder.

The authors would like to thank S. A. Sunshine, T. Siegrist, A. Jayaraman, G. A. Kourouklis, K. B. Lyons, B. Batlogg, M. Schluter, and D. W. Murphy for stimulating discussions.

*Permanent address: Institut für Nukleare Festkörperphysik, Kernforschungszentrum Karlsruhe, V-7500 Karlsruhe 1, Federal Republic of Germany.

¹M. Stavola, D. M. Krol, W. Weber, S. A. Sunshine, A. Jayaraman, G. A. Kourouklis, R. J. Cava, and E. A. Rietman, *Phys. Rev. B* **36**, 850 (1987).

²B. Batlogg, R. J. Cava, A. Jayaraman, R. B. vanDover, G. A. Kourouklis, S. A. Sunshine, D. W. Murphy, L. W. Rupp, H. S. Chen, A. White, K. T. Short, A. M. Muijsce, and E. A. Rietman, *Phys. Rev. Lett.* **58**, 2333 (1987).

³R. J. Hemley and H. K. Mao, *Phys. Rev. Lett.* **58**, 2337 (1987).

⁴Liu Ran, R. Merlin, M. Cardona, H. J. Mattausch, W. Bauhofer, A. Simon, F. Garcia-Alvarado, E. Moran, M. Vallet, J. M. Gonzalez-Calbet, and M. A. Alario, *Solid State Commun.* **63**, 839 (1987).

⁵H. Rosen, E. M. Engler, T. C. Strand, V. Y. Lee, and D. Bethune, *Phys. Rev. B* **36**, 726 (1987).

⁶R. M. Macfarlane, H. Rosen, and H. Seki, *Solid State Commun.* **63**, 831 (1987).

⁷K. B. Lyons, S. H. Liou, M. Hong, H. S. Chen, J. R. Kwo, and T. J. Negran, *Phys. Rev. B* **36**, 5592 (1987).

⁸Z. Iqbal, S. W. Steinhäuser, A. Bose, N. Apollini, and H. Eckhardt, *Phys. Rev. B* **36**, 2283 (1987).

⁹G. A. Kourouklis, A. Jayaraman, B. Batlogg, R. J. Cava,

M. Stavola, D. M. Krol, E. A. Rietman, and L. F. Schneemeyer, preceding paper *Phys. Rev. B* **36**, 8320 (1987).

¹⁰P. K. Gallagher, H. M. O'Bryan, S. A. Sunshine, and D. W. Murphy, *Mater. Res. Bull.* **22**, 995 (1987).

¹¹T. Siegrist, S. A. Sunshine, D. W. Murphy, R. J. Cava, and S. M. Zahurak, *Phys. Rev. B* **35**, 7137 (1987).

¹²A. Santoro, S. Miraglia, F. Beech, S. A. Sunshine, D. W. Murphy, L. F. Schneemeyer, and J. V. Waszczak, *Mater. Res. Bull.* **22**, 1007 (1987).

¹³A. W. Hewat, J. J. Capponi, C. Chailout, M. Marezio, and E. A. Hewat, *Nature* (to be published).

¹⁴R. J. Cava, B. Batlogg, C. H. Chen, E. A. Rietman, S. M. Zahurak, and D. Werder, *Phys. Rev. B* **36**, 5719 (1987).

¹⁵L. F. Schneemeyer, J. V. Waszczak, T. Siegrist, R. B. van Dover, L. W. Rupp, B. Batlogg, R. J. Cava, and D. W. Murphy, *Nature* **328**, 601 (1987).

¹⁶Y. Le Page, T. Siegrist, S. A. Sunshine, L. F. Schneemeyer, D. W. Murphy, S. M. Zahurak, J. V. Waszczak, W. R. McKinnon, J. M. Tarascon, G. W. Hull, and L. H. Greene, *Phys. Rev. B* **36**, 3617 (1987).

¹⁷S. Kosinski, D. M. Krol, J. R. Simpson, and J. B. MacChesney, *J. Non-Cryst. Solids* (to be published).

¹⁸See, e.g., M. V. Klein, in *Superconductivity in d- and f-Band Metals*, edited by W. Buckel and W. Weber (Kernforschungszentrum, Karlsruhe, 1982), p. 39.